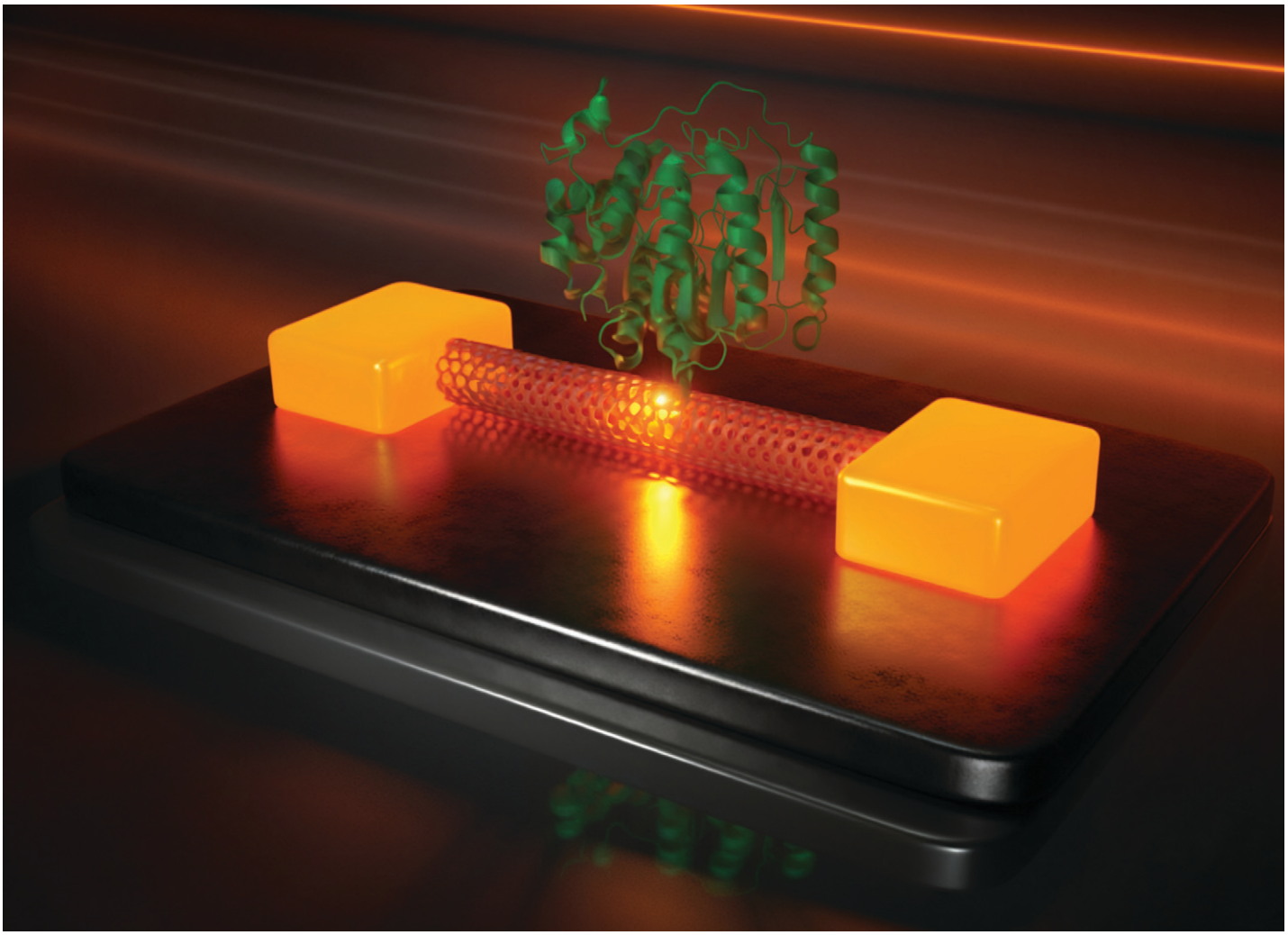

Showcasing research from Professor Yongki Choi's laboratory, Department of Physics, North Dakota State University, Fargo, North Dakota, United States of America.

Substrate structure modulates the catalytic dynamics of HDAC8 at the single-molecule level

This work explores how subtle molecular modifications can fine-tune the performance of an enzyme critical to cellular regulation. Using nanoscale electronic sensors, the catalytic motions of individual histone deacetylase 8 (HDAC8) molecules are monitored in real time. The study shows that chemical substitutions and small activating molecules can work together to stabilize efficient enzyme shapes and boost activity. These findings reveal how molecular design and dynamic motion intersect to control enzyme behavior at the single-molecule level.

Cover image created with Blender and modified using AI

Image reproduced by permission of Yongki Choi from *Catal. Sci. Technol.,* 2025, **15**, 7324.

As featured in:

See Yongki Choi *et al.*, *Catal. Sci. Technol.*, 2025, **15**, 7324.

ROYAL SOCIETY OF CHEMISTRY

rsc.li/catalysis

Registered charity number: 207890

Catalysis Science & Technology

ROYAL SOCIETY OF CHEMISTRY

COMMUNICATION

View Article Online
View Journal | View Issue

Cite this: *Catal. Sci. Technol.*, 2025, **15**, 7324

Received 16th June 2025,
Accepted 20th October 2025

DOI: 10.1039/d5cy00729a

rsc.li/catalysis

Substrate structure modulates the catalytic dynamics of HDAC8 at the single-molecule level

Seungyong You,[a] Sakurako Tani,[a] Sanku Mallik,[b] Zhongyu Yang,[c] Mohiuddin Quadir[d] and Yongki Choi*[a]

Understanding how substrate structure alters an enzyme's conformational landscape is central to catalyst design. Using single-molecule electronic sensors, we reveal how substitutions on an HDAC8 substrate modulate the enzyme's underlying catalytic dynamics. We demonstrate that a trifluoroacetyl group accelerates catalysis, while a Boc cap and an allosteric activator synergistically simplify the kinetic pathway by stabilizing productive conformations. These findings provide direct, real-time insight into how substrate-induced conformational dynamics control enzyme catalysis.

Histone deacetylase 8 (HDAC8) is a metalloenzyme that catalyzes the removal of acetyl groups from lysine residues on histone and non-histone substrates, regulating gene expression and protein function.[1] While HDAC8 has been studied extensively in biological contexts,[2,3] understanding how ligand modifications regulate its catalytic activity remains a central question in enzymatic catalysis. HDAC8 represents a dynamic catalytic system where conformational flexibility plays a critical role in substrate binding and turnover efficiency.[1,4]

Conventional drug design often relies on static crystallographic snapshots of enzyme-ligand complexes; however, for highly flexible enzymes like HDAC8, dynamic conformational states significantly influence catalysis.[5,6] The active site of HDAC8 includes multiple subregions (*i.e.*, metal-binding, linker, and cap regions) which can be selectively engaged by ligands to modulate activity.[7] Traditional ensemble assays typically average over these conformational states, limiting mechanistic understanding of how ligands control catalytic pathways. In this work, we employ label-free single-molecule electronic sensors based on single-walled carbon nanotube field-effect transistors (SWNT-FETs) to directly monitor HDAC8 catalytic activity in real-time under various ligand modifications.[8–12] A single-molecule HDAC8 nanosensor is depicted in Fig. 1a, where HDAC8 is tethered *via* N-terminal His_6-tag through a pyrene-iminodiacetate–Cu^{2+} linker, and the attachment is distal to the active site. This N-terminal tag is distal to the catalytic site, and because the observed dynamics are highly ligand-dependent, the tag is not considered a source of experimental artifact. Atomic force microscopy confirmed the attachment of a single HDAC8 molecule on the SWNT (Fig. 1b). In the nanosensor, conformational motions of HDAC8 enzyme modulate the nanosensor conductance *via* electrostatic gating.[11,12] This enables continuous, long-duration monitoring of HDAC8 motions and catalytic events, overcoming the temporal limitations of conventional optical assays. Using this approach, we captured HDAC8's conformational dynamics during deacetylation of different substrate analogs.

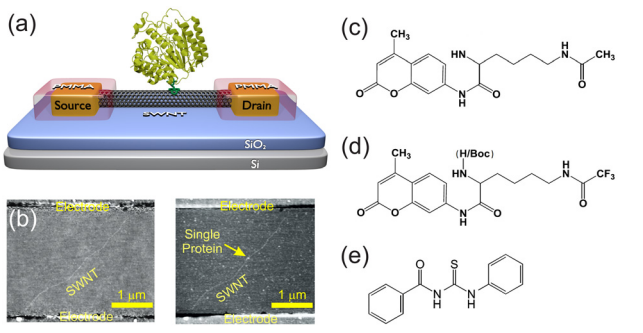

Fig. 1 (a) Schematic of the single-HDAC8 nanosensor. (b) AFM images of the sensor before and after attachment of a single HDAC8 molecule. Chemical structures of (c) acetyl-lysine–coumarin (AL–AMC), (d) trifluoroacetyl-lysine–coumarin in the absence (TFAL–AMC) and presence (Boc-TFAL–AMC) of a Boc protected α-amine, and (e) the activator *N*(phenylcarbothiol)benzamide (ACT).

[a] *Department of Physics, North Dakota State University, Fargo, North Dakota 58108, USA. E-mail: yongki.choi@ndsu.edu*
[b] *Department of Pharmaceutical Sciences, North Dakota State University, Fargo, North Dakota 58108, USA*
[c] *Department of Chemistry and Biochemistry, North Dakota State University, Fargo, North Dakota 58108, USA*
[d] *Department Coatings and Polymeric Materials, North Dakota State University, Fargo, North Dakota 58108, USA*

To uncover how ligand modifications and allosteric effectors modulate HDAC8 catalysis, this work focuses on two strategic ligand alterations: a trifluoroacetyl-lysine moiety in a substrate analog, and an α-amine *tert*-butyloxycarbonyl (Boc) protecting group appended as a distal cap on the substrate (Fig. 1c and d). The trifluoroacetyl substitution is a strategy used to probe catalysis; the strong electron-withdrawing nature of the trifluoromethyl group increases the carbonyl's electrophilicity, facilitating nucleophilic attack and stabilizing the tetrahedral intermediate formed during the reaction. The bulky Boc group, in contrast, is positioned at the substrate's N-terminus (outside the catalytic core) to engage the enzyme's outer pocket or exosite. This distal interaction can provide additional binding energy and orient the substrate for more efficient turnover. Thus, catalytic activities of HDAC8 with a minimal acetyl-lysine coumarin substrate (AL–AMC), the transition-state mimic trifluoroacetyl-lysine analog (TFAL–AMC), Boc-appended derivative of the trifluoroacetyl substrate (Boc-TFAL–AMC) were examined and compared. In addition to these substrate modifications, the effect of the potent activator, *N*(phenylcarbothiol)benzamide (ACT; Fig. 1e) was also examined. ACT is known to enhance catalytic activity in bulk assays by engaging active site residues, understood to involve two distinct regions within the catalytic tunnel (*i.e.*, the entrance and an inner pocket).[13,14] By monitoring single HDAC8 molecules with and without ACT, we directly observed how this specific mode of active-site engagement cooperates with distal substrate anchoring to allosterically modulate the enzyme's conformational landscape.

All measurements were performed at high substrate concentration (100 μM) under steady-state single-enzyme conditions, where substrate depletion is negligible over the recording window. While K_M values may differ among analogs, our comparative conclusions rely on dwell-time statistics (τ_{hi} and τ_{lo}) and remain robust to modest differences from full saturation. Fig. 2a–e compare the single-molecule traces obtained with the substrates. In the absence of substrate (buffer alone; 25 mM HEPES, 100 mM NaCl, 1 mM TCEP, pH 7.5), the device current remained at a steady baseline, indicating a stable enzyme conformation with no catalytic activity (Fig. 2a). Upon introducin1g an acetyl-lysine substrate, the real-time current $\Delta I(t)$ displayed distinct downward deflections (Fig. 2b–e), indicating the formation of an HDAC8–substrate complex. The conductance changes are consistent with electrostatic gating by charged residues on the catalytic loop (for example, R37 and H42 as candidate contributors) that approach the nanotube during loop opening. We present a charge-displacement model (Fig. S1) based on open/closed crystal structures to illustrate this mechanism, while recognizing that alternative loop motions could also yield the observed polarity and amplitude.[15,16] Accordingly, the high-current baseline corresponds to the enzyme's closed-loop state, and each downward pulse correlates with a transient open-loop conformation. This assignment is supported by prior single-molecule nanosensor studies[8,11,17] and by bulk HDAC8 kinetics in which the frequency of loop-opening spikes in our recordings matches the ensemble k_{cat},[18] confirming our nanosensor readout directly tracks HDAC8's conformational motions and catalysis in real time. Furthermore, the repetitive, sustained cycling is a signature of enzymatic turnover, and the frequency of these events directly correlates with the known catalytic efficiencies of the substrates, confirming that the motions are coupled to productive catalysis.

Single-molecule recordings revealed that TFAL–AMC undergoes frequent and periodic current fluctuations, indicative of robust catalytic turnover by HDAC8 (Fig. 2b). These dynamics are consistent with ensemble kinetic measurements, which showed that TFAL–AMC exhibits a high

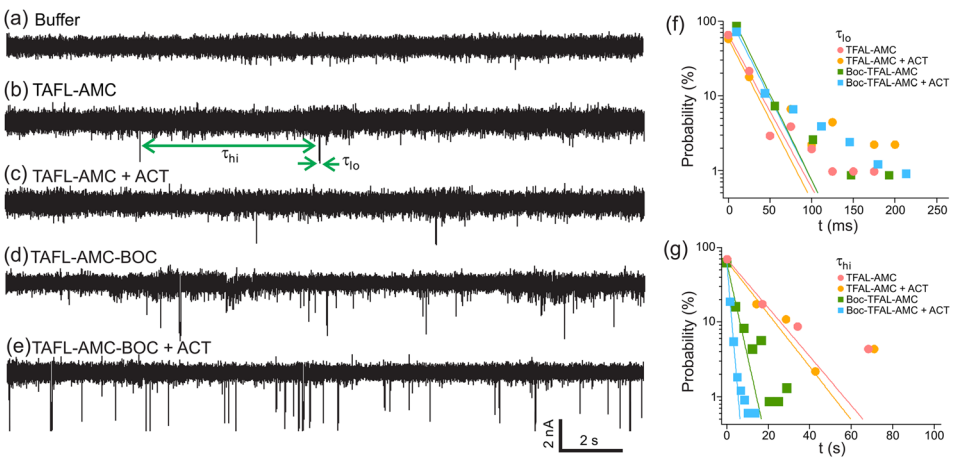

Fig. 2 Comparison of HDAC8 loop dynamics in the presence of (a) buffer, (b) TFAL–AMC, (c) TFAL–AMC with ACT, (d) Boc-TFAL–AMC, and (e) Boc-TFAL–AMC with ACT. A data trace for AL–AMC is not shown as its rare catalytic events are not visually illustrative (see Fig. S2). Dwell time distributions of (f) low-current (τ_{lo}) and (g) high-current (τ_{hi}) states, corresponding to the open-loop and closed-loop conformations, respectively. These plots are normalized probability distributions of all measured dwell times for each condition. The solid lines in (f) and (g) are single-exponential fits to the dwell time distributions, where a straight line on these semi-log plots indicates a single rate-limiting step.

catalytic rate (k_{cat} = 5 × 10^{-2} s^{-1}) relative to the minimal substrate (AL–AMC). This enhancement is attributed to the electron-withdrawing trifluoromethyl group, which increases the carbonyl's electrophilicity and thereby accelerates catalysis. In contrast, AL–AMC produced only rare current transitions over several minutes under identical single-molecule conditions (Table 1), indicating much slower turnover (k_{cat} = 6.7 × 10^{-3} s^{-1}). While this single-molecule rate differs from the ensemble k_{cat} estimate (4 × 10^{-4} s^{-1}), the discrepancy can be attributed to static heterogeneity, as our single-molecule method inherently selects active enzymes, whereas ensemble assays average over all molecules, including inactive ones. A complete summary of the single-molecule kinetic parameters is presented in Table 1. The data reveal a clear trend: while the minimal substrate, AL–AMC, is turned over very slowly, the addition of the trifluoroacetyl group, the Boc cap, and the activator each progressively accelerates catalysis. The following sections will dissect the specific kinetic steps responsible for these enhancements.

Introducing the bulky Boc cap on the TFAL substrate led to a further acceleration of catalysis (Fig. 2d). Single-molecule trajectories of HDAC8 with Boc-TFAL–AMC revealed much more frequent catalytic current spikes than with TFAL–AMC alone (Fig. 2b). The average waiting time between catalytic spikes (the high-current dwell time, τ_{hi}) was dramatically reduced by the Boc modification. For TFAL–AMC, the mean closed-loop dwell time τ_{hi} was about 13.7 s (no activator), whereas with Boc-TFAL–AMC it dropped to 3.5 s. This corresponds to an approximately 3.7-fold increase in turnover rate ($k = 1/(\tau_{hi} + \tau_{lo})$) due to the Boc group. Notably, the duration of each low-current state ($\tau_{lo} \approx 20$ ms) was unchanged across ligands, whereas the high-current state (τ_{hi}) shortened substantially with Boc and further with ACT. Thus, the Boc cap accelerates pre-chemical steps (encounter/orientation and loop opening) without altering the chemical step, and ACT cooperates with Boc to further simplify/accelerate the pre-chemical pathway. We conclude that the Boc moiety likely engages HDAC8's exosite or entry region, providing additional binding interactions that tether the substrate in a productive orientation. By pre-organizing the enzyme–substrate complex, the Boc cap minimizes the conformational search, allowing the catalytic loop to open more readily. While a direct binding affinity (K_d) was not measured, this observation of a kinetically accelerated pre-chemical step provides strong functional evidence for the Boc group's role in substrate recruitment and orientation. This is analogous to previous observations that appending bulky cap groups to HDAC inhibitors or adding C-terminal basic residues to peptide substrates can significantly enhance binding affinity and catalytic rate by interacting with surface residues outside the catalytic tunnel.[7,19] In addition, thermodynamic analysis based on a two-state Boltzmann model support that the Boc group reduces the effective free-energy difference between the closed and open states ($\Delta E = k_B T \ln(\tau_{lo}/\tau_{hi})$) by 41%, indicating a flatter energy landscape that makes it easier for the enzyme to sample the catalytically competent conformation (Table 1).

Next, the role of the allosteric activator ACT on HDAC8's kinetics with each substrate was examined (Fig. 2c and e). Interestingly, the impact of ACT was dependent on the substrate's structure. In the case of the TFAL–AMC substrate, introducing ACT had little to no effect on the single-molecule dwell times, both mean durations, τ_{lo} and τ_{hi}, remained essentially the same with or without the activator (≈21 ms and 12–14 s, respectively), yielding an unchanged overall turnover rate (Table 1). This suggests that when the substrate already carries the highly electrophilic trifluoroacetyl group, HDAC8 operates near its optimal catalytic efficiency, and further allosteric modulation provides no additional benefit. The enzyme's rate-limiting conformational steps with TFAL–AMC (such as loop motions to align the substrate) are not significantly accelerated by ACT, perhaps because TFAL–AMC lacks robust anchoring at the entry site, leaving ACT with no cooperative partner to stabilize the complex.

With both Boc and ACT present, HDAC8 displayed a dramatically shortened waiting time between catalytic events (τ_{hi} = 1.3 s, compared to 3.5 s). This corresponds to an additional 2.6-fold increase in turnover frequency on top of the Boc enhancement alone. In other words, ACT and Boc together accelerated the catalysis by nearly an order of magnitude relative to the unmodified TFAL substrate. Notably, under these conditions the distribution of closed-state dwell times also became significantly tighter (as discussed below), approaching the characteristics of a single-step process. The data indicate that ACT selectively stabilizes or promotes a productive conformation of the enzyme–

Table 1 Single-molecule kinetic parameters for various substrates[a]

Ligands	τ_{lo} (ms)		r_{lo}	τ_{hi} (s)		r_{hi}	k^c (s^{-1})	ΔE^d (kcal mol^{-1})
AL–AMC	15.8	±4.62[b]		150.0	±73.82[b]		0.0067	
AL–AMC + ACT	37.1	±48.1[b]		127.3	±76.0[b]		0.0079	
TFAL–AMC	21.3	±0.81	1.06 ± 0.25	13.7	±0.85	0.62 ± 0.34	0.073 ± 0.005	3.88 ± 0.04
TFAL–AMC + ACT	20.8	±0.57	1.02 ± 0.39	12.2	±1.77	0.71 ± 0.33	0.082 ± 0.012	3.82 ± 0.09
Boc-TFAL–AMC	18.9	±0.62	1.03 ± 0.17	3.47	±0.37	0.84 ± 0.17	0.287 ± 0.031	3.13 ± 0.06
Boc-TFAL–AMC + ACT	19.7	±1.62	0.99 ± 0.14	1.32	±0.027	0.92 ± 0.14	0.746 ± 0.016	2.52 ± 0.05

[a] Average values ± standard deviation. [b] Arithmetic average. [c] Turnover rate calculated as $k = 1/(\tau_{hi} + \tau_{lo})$. [d] Apparent free-energy difference calculated as $\Delta E = k_B T \ln(\tau_{lo}/\tau_{hi})$. Uncertainty in derived parameters (k, ΔE) reflects the propagation of errors from the directly measured τ values.

substrate complex, particularly when the substrate is already partially stabilized by the Boc group. ACT's engagement within the active site tunnel helps to align internal catalytic residues and optimize catalytic geometry; however, this optimization by ACT becomes especially effective for accelerating catalysis when the substrate is concurrently anchored externally by the Boc group. Thus, with the substrate tethered by Boc, ACT's influence on the active site can more efficiently lock the enzyme–substrate complex into the active conformation, greatly expediting catalysis. This cooperative mechanism is evident in the free-energy analysis. When both ACT and Boc are present, the ΔE between closed and open states was reduced by 21% relative to Boc-TFAL–AMC alone, indicating ACT further flattens the energy landscape toward the active state. Such a synergistic effect, arising from ACT's active site interactions coupled with distal substrate anchoring by Boc, highlights that HDAC8's activation is ligand-dependent and tunable *via* multi-site interactions.

The activator's influence on the poor substrate like AL–AMC was limited. For the minimal AL–AMC substrate, very few catalytic events were observed to begin with, and the addition of ACT did not significantly increase the overall turnover, though we did notice a slight lengthening of the rare τ_{lo} events when ACT was present. This minor effect suggests that ACT may stabilize the enzyme–substrate encounter complex even for suboptimal ligands, but if the ligand is intrinsically unable to attain a productive conformation or stabilize the catalytic transition state, then prolonged binding has little impact. These observations support that productive catalysis in HDAC8 arises from a specific subset of enzyme–ligand conformations, and both ligand modifications and activators function by favoring those productive subsets.

To quantitatively dissect the kinetic pathways underlying HDAC8's activity, we analyzed the statistical distribution of dwell times in the closed and open states (Fig. 2f and g). The brief open-state durations (τ_{lo}) followed a simple exponential distribution with mean (τ_{lo}) values approximately 20 ms across all substrates, with or without Boc and ACT. This indicates that once HDAC8 achieves the catalytically competent, open-loop conformation with the substrate properly positioned, the time to hydrolyze the acetyl-lysine and release product is essentially constant. Consequently, the chemistry (*i.e.*, cleavage of the acetyl group and subsequent product dissociation) likely proceeds through a single rate-limited step that is insensitive to the ligand's structural modifications. This observation aligns with classical enzyme kinetics, where the inherent chemical transformation and rapid product release are determined by the enzyme's active site and the substrate's acyl bond, factors minimally influenced by a distal Boc group or allosteric effector binding. It also supports our earlier assignment that τ_{lo} corresponds to the actual catalytic event (deacetylation), as expected for a single-exponential process.

The mean-normalized variance of the two dwell times, $r = \sigma^2/\langle\tau\rangle^2$, shows that $r_{lo} \approx 1$, consistent with τ_{lo} arising from a single-step Poisson process and first-order reaction.[8,20] In contrast, the distributions of the closed-state (τ_{hi}) were highly sensitive to ligand modifications and showed deviations from single-exponential behavior, indicating multi-step kinetics. The mean (τ_{hi}) spanned a broad range, from 13.7 s (TFAL–AMC, no activator) to 1.3 s (Boc-TFAL–AMC with activator), reflecting how different ligands accelerate the enzyme. For TFAL–AMC without activator, the distribution of τ_{hi} was broad, with a variance-to-mean ratio r_{hi} on the lower end of our observed range (r_{hi} = 0.6–0.7). Such an r_{hi} value suggests that two or more rate-limiting microsteps underlie the closed to open transition. These microsteps can be interpreted as mechanistic stages of enzyme–substrate recognition: (i) an initial desolvation and binding of the substrate to HDAC8 (formation of a loose encounter complex), followed by (ii) immobilization and orientational adjustments of the substrate in the active site (loop reconfiguration or packing the ligand into a productive pose). Only after these steps does the enzyme attain the fully productive conformation (open loops) corresponding to the catalytic event. This mode is supported by prior analyses of enzyme binding mechanisms and by the widely accepted idea that HDAC8 including many enzymes fluctuates among a spectrum of conformational substates, of which only a subset are capable of productive catalysis.[5,6] Our single-molecule results provide evidence for such behavior: the enzyme spends a long and variable time in the closed state because it may undergo several attempts to bind and arrange the substrate correctly before a successful catalytic turnover occurs.

When ligand modifications that favor productive binding were introduced, the τ_{hi} distributions became narrower and more shifted toward shorter times. Boc-TFAL–AMC, for instance, not only had a smaller (τ_{hi}), but its closed-state variance r_{hi} increased towards unity ($r_{hi} \approx$ 0.8–0.9). This trend of r_{hi} moving closer to 1 indicates that the waiting time is becoming more single exponential, implying that the underlying multi-step process has been simplified or reduced in number of steps. The Boc group likely eliminates or makes one of the binding steps highly efficient. The addition of the activator to Boc-TFAL–AMC further accelerates the process. The r_{hi} approaches to unity, within error, suggesting that the combination of substrate anchoring and allosteric activation has simplified the kinetic pathway. This shift renders the pre-chemical steps non-rate-limiting, causing the overall turnover to be kinetically dominated by a single rate-limiting step, as evidenced by the distribution approaching single-exponential behavior. This cooperative behavior points to allosteric communication between the enzyme's surface binding site and its active site.

Conclusions

In summary, this single-molecule study reveals how ligand modifications synergistically modulate HDAC8 catalysis by altering conformational dynamics. The trifluoroacetyl analog

accelerates the chemical deacetylation step, while substrate capping (Boc group) and allosteric activation (ACT) stabilize productive enzyme conformations that increase turnover frequency. These multi-site interactions reshape the free-energy landscape of HDAC8, leading to efficient catalysis. These insights may also inform future design of bifunctional ligands or activators that exploit multi-site interactions to optimize catalytic efficiency. We acknowledge that this study does not include a direct measurement of equilibrium binding affinity (K_d) for the modified substrates. Future ensemble studies measuring K_d and Michaelis–Menten constants (K_M), together with docking and MD simulations, would complement the single-molecule kinetic data and provide a more complete thermodynamic and kinetic picture of HDAC8 catalysis.

Author contributions

Study concept and design (S. Y., Y. C.); data acquisition, analysis, or interpretation (S. Y., S. T., S. M., Z. Y., M. Q., Y. C.); the manuscript was written through the contributions of all authors. All authors have approved the final version of the manuscript.

Conflicts of interest

There are no conflicts to declare.

Data availability

The data supporting this article have been included as part of the SI. The SI contains detailed experimental protocols, device fabrication and measurement parameters, and the signal transduction model that supports the generation and interpretation of the data presented in this study. Key data are summarized in the figures and Table 1 of the main manuscript. Supplementary information: materials and methods, device fabrication and measurements, and signal transduction. See DOI: https://doi.org/10.1039/d5cy00729a.

Acknowledgements

We thank members of D. K. Srivastava's laboratory for supplying HDAC8. This research was supported by the National Science Foundation (NSF CBET-2317111).

Notes and references

1 P. M. Lombardi, K. E. Cole, D. P. Dowling and D. W. Christianson, *Curr. Opin. Struct. Biol.*, 2011, **21**, 735–743.
2 A. Mai, S. Massa, D. Rotili, I. Cerbara, S. Valente, R. Pezzi, S. Simeoni and R. Ragno, *Med. Res. Rev.*, 2005, **25**, 261–309.
3 J. E. Bradner, N. West, M. L. Grachan, E. F. Greenberg, S. J. Haggarty, T. Warnow and R. Mazitschek, *Nat. Chem. Biol.*, 2010, **6**, 238–243.
4 M. A. Deardorff, M. Bando, R. Nakato, E. Watrin, T. Itoh, M. Minamino, K. Saitoh, M. Komata, Y. Katou and D. Clark, *et al.*, *Nature*, 2012, **489**, 313–317.
5 C. Yan, Z. Xiu, X. Li, S. Li, C. Hao and H. Teng, *Proteins: Struct., Funct., Bioinf.*, 2008, **73**, 134–149.
6 K. Henzler-Wildman and D. Kern, *Nature*, 2007, **450**, 964–972.
7 R. K. Singh, T. Suzuki, T. Mandal, N. Balsubramanian, M. Haldar, D. J. Mueller, J. A. Strode, G. Cook, S. Mallik and D. K. Srivastava, *Biochemistry*, 2014, **53**, 7445–7458.
8 Y. Choi, I. S. Moody, P. C. Sims, S. R. Hunt, B. L. Corso, G. A. Weiss and P. G. Collins, *Science*, 2012, **335**, 319–324.
9 Y. Choi, I. S. Moody, P. C. Sims, S. R. Hunt, B. L. Corso, D. E. Seitz, L. C. Blaszcazk, P. G. Collins and G. A. Weiss, *J. Am. Chem. Soc.*, 2012, **134**, 2032–2035.
10 K. M. Pugliese, O. T. Gul, Y. Choi, T. J. Olsen, P. C. Sims, P. G. Collins and G. A. Weiss, *J. Am. Chem. Soc.*, 2015, **137**, 9587–9594.
11 S. You, J. Froberg, J. Yu, M. Haldar, A. Sedigh, S. Mallik, D. K. Srivastava and Y. Choi, *Chem. Commun.*, 2017, **53**, 3307–3310.
12 Y. Choi, T. J. Olsen, P. C. Sims, I. S. Moody, B. L. Corso, M. N. Dang, G. A. Weiss and P. G. Collins, *Nano Lett.*, 2013, **13**, 625–631.
13 R. K. Singh, T. Mandal, N. Balsubramanian, T. Viaene, T. Leedahl, N. Sule, G. Cook and D. K. Srivastava, *Bioorg. Med. Chem. Lett.*, 2011, **21**, 5920–5923.
14 R. K. Singh, K. Cho, S. K. Padi, J. Yu, M. Haldar, T. Mandal, C. Yan, G. Cook, B. Guo, S. Mallik and D. K. Srivastava, *J. Biol. Chem.*, 2015, **290**, 6607–6619.
15 C. Decroos, D. J. Clausen, B. E. Haines, O. Wiest, R. M. Williams and D. W. Christianson, *Biochemistry*, 2015, **54**, 2126–2135.
16 M. B. Kunze, D. W. Wright, N. D. Werbeck, J. Kirkpatrick, P. V. Coveney and D. F. Hansen, *J. Am. Chem. Soc.*, 2013, **135**, 17862–17868.
17 Y. Choi, T. J. Olsen, P. C. Sims, I. S. Moody, B. L. Corso, M. N. Dang, G. A. Weiss and P. G. Collins, *Nano Lett.*, 2013, **13**, 625–631.
18 R. K. Singh, N. Lall, T. S. Leedahl, A. McGillivray, T. Mandal, M. Haldar, S. Mallik, G. Cook and D. K. Srivastava, *Biochemistry*, 2013, **52**, 8139–8149.
19 Z. A. Gurard-Levin and M. Mrksich, *Biochemistry*, 2008, **47**, 6242–6250.
20 S. O. Woo, M. Oh, L. Alhalhooly, J. Farmakes, A. J. Rajapakse, Z. Yang, P. G. Collins and Y. Choi, *J. Phys. Chem. B*, 2021, **125**, 5750–5756.

